

Shocks and Excitation Dynamics in a Driven Diffusive Two-Channel System

Vladislav Popkov¹ and Gunter M. Schütz¹

Received November 4, 2002; accepted February 5, 2003

We consider classical hard-core particles hopping stochastically on two parallel chains in the same or opposite directions with an inter- and intra-chain interaction. We discuss general questions concerning elementary excitations in these systems, shocks and rarefaction waves. From microscopical considerations we derive the collective velocities and shock stability conditions. The findings are confirmed by comparison to Monte Carlo data of a multi-parameter class of simple two lane driven diffusion models, which have the stationary state of a product form on a ring. Going to the hydrodynamic limit, we point out the analogy of our results to the ones known in the theory of differential equations of two conservation laws. We discuss the singularity problem and find a dissipative term that selects the physical solution.

KEY WORDS: Asymmetric exclusion process; shock; hydrodynamic limit; system of two conservation laws.

1. INTRODUCTION

Driven many-particle systems have been the topic of numerous studies in recent years.⁽¹⁾ Despite relatively simple formulation, they have rich dynamic features and phase behaviour and proved to be useful testing ground in nonequilibrium physics. Among the new phenomena they highlight are, for instance, nonequilibrium boundary-driven phase transitions,⁽²⁾ spontaneous symmetry breaking,⁽³⁾ and others. From the mathematical viewpoint, dynamics of many nonequilibrium particle models are Markov

¹ Institut für Festkörperforschung, Forschungszentrum Jülich, 52425 Jülich, Germany; e-mail: {v.popkov;g.schuetz}@fz-juelich.de

processes. The hydrodynamic limit of the latter contributes to the theory of the differential equations of conservation laws.^(4,5)

If a driven system consists of particles of only one type (one species case), its dynamics can be well understood in terms of elementary excitations.⁽⁶⁾ Pursuing further the approach of ref. 6, one can explain and subsequently predict the stationary phase diagram for systems with arbitrary current-density relation.⁽⁷⁾ However, multi-species models (i.e., those having two or more different particle types, each conserved separately) have so far eluded careful examination. For very recent work, see ref. 8. Earlier studies indicate a phase diagram much richer compared to the one species case, including the existence of new phases and phase transitions.^(3,9) The dynamic properties that lead to these phase transitions were not studied.

The present paper presents a step towards understanding of how elementary excitations behave in a driven system with two species. For that purpose, we propose a new class of models for which the stationary state has a simple form on a ring. We study them by analytical means and supplement our findings with numerical Monte Carlo simulations and mean field calculations.

The paper is organized as follows. In Section 2 we define the model and describe the stationary state on a ring. In Section 3 we describe how a local perturbation spreads and obtain the eigenvalue equation for the collective velocities. In Section 4 the dynamical evolution of a system with step-like initial condition (Riemann problem) is considered. We discuss shocks and rarefaction waves and their stability. A comparison with partial differential equations obtained by taking the continuum limit of the microscopic model is given in Section 5. Some technical details concerning the derivation of the stationary flux and the spreading of a local perturbation can be found in the Appendices.

2. THE MODEL

Our model consists of two parallel chains, chain A and chain B. Each chain contains hard-core particles which hop randomly to the nearest right or left site if it is empty. Hopping between the chains is not allowed as well as occupation of a site by more than one particle (exclusion principle). The hopping rate in one chain depends on the configuration of the neighbouring sites in the other chain so that for each chain one has the eight possibilities shown in Fig. 1. For the sake of simplicity, we consider either the symmetric system (when the hopping rates on the both chains are the same), or the antisymmetric system (when the rates on the different chains are left-right reflected).

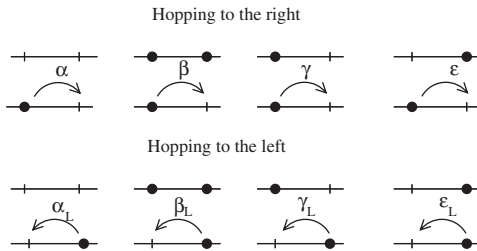


Fig. 1. The eight allowed elementary hopping processes for the first chain, and their rates. In the study we choose the rates for the second chain either to be the same, Eq. (1) or to be antisymmetric (reflected with respect to the first chain), see Eq. (2).

The stationary state for a periodic system has a simple form (3) if and only if the hopping rates (Fig. 1) satisfy the condition

$$\alpha - \alpha_L + \beta - \beta_L = 2(\gamma - \gamma_L e^\nu) = 2(\epsilon e^\nu - \epsilon_L) \quad (1)$$

for the symmetric model and

$$\alpha - \alpha_L = \beta - \beta_L = \gamma e^{-\nu} - \gamma_L = \epsilon - \epsilon_L e^{-\nu} \quad (2)$$

for the antisymmetric one. Here ν is an arbitrary real number. For a ring of L sites, the stationary probability of the configuration $P_{n_1, n_2, \dots, n_L}^{m_1, m_2, \dots, m_L}$ then has the product form

$$P_{n_1, n_2, \dots, n_L}^{m_1, m_2, \dots, m_L} = Z^{-1} \prod_{k=1}^L \exp(-\nu n_k m_k). \quad (3)$$

Here n_k, m_k are occupation numbers for the A- and the B-chain respectively, i.e., $n_k = 0$ ($n_k = 1$), if the k th site on the A-chain is empty (occupied by a particle). Z is a normalization factor, analogous to the partition function in statistical mechanics. One can check that Eqs. (1)–(3) satisfy the stationarity requirements by considering gain and loss processes from and to an arbitrary configuration like it is done in ref. 10. One sees from Eq. (3) that different sites $k \neq j$ are uncorrelated. If in addition $\nu = 0$, then the adjacent pairs of sites are also uncorrelated.

For demonstration purposes, we shall take general symmetric model (1) and simplify it further: firstly, we forbid all backward hoppings and secondly, we set $\nu = 0$. With the above restrictions, the hopping rates satisfy $\alpha + \beta = 2\gamma = 2\epsilon$, and can be parametrized by only one parameter β :

$$\alpha = 1; \quad \gamma = \epsilon = (1 + \beta)/2; \quad \alpha_L = \beta_L = \gamma_L = \epsilon_L \equiv 0. \quad (4)$$

Since the rates must not be negative, β is in the range $0 \leq \beta < \infty$. $\beta = 1$ corresponds to the model with no interaction between the chains, called totally asymmetric exclusion process (TASEP).^(11,12) The other choice of the rates $\alpha = \beta = \gamma \neq \epsilon$, $\alpha_L = \beta_L = \gamma_L = \epsilon_L \equiv 0$ was considered in ref. 9. With the choice (4), stationary fluxes j^A, j^B of particles on the chains A and B are readily computed to be

$$\begin{aligned} j^A(\rho^A, \rho^B) &= \rho^A(1 - \rho^A)(1 + (\beta - 1)\rho^B) \\ j^B(\rho^A, \rho^B) &= \rho^B(1 - \rho^B)(1 + (\beta - 1)\rho^A). \end{aligned} \quad (5)$$

For completeness, we list here exact analytic expressions for the flux in general case (see Appendix A for details). For symmetric hopping rates (1),

$$\begin{aligned} j_{\text{sym}}^A(\rho^A, \rho^B) &= (\epsilon - \gamma_L)(e^\nu - 1) f_{AB} f_{BA} + (\alpha - \alpha_L - \gamma + \epsilon_L)(1 - \rho^A) f_{AB} \\ &\quad + (\beta - \beta_L - \gamma + \epsilon_L) \rho^A f_{BA} + (\gamma - \epsilon_L) \rho^A(1 - \rho^A) \\ j_{\text{sym}}^B(\rho^A, \rho^B) &= j_{\text{sym}}^A(\rho^B, \rho^A) \end{aligned} \quad (6)$$

where f_{AB} (f_{BA}) is the stationary probability to find a particle on chain A (B) and a hole on the adjacent site on the other chain. This probability can be obtained from the stationary distribution (3),

$$\begin{aligned} f_{AB} &= \frac{2\rho^A(1 - \rho^B)}{1 + \mathcal{F}_{AB} - \mathcal{F}_{BA} + \sqrt{1 + (\mathcal{F}_{AB} - \mathcal{F}_{BA})^2 - 2\mathcal{F}_{AB} - 2\mathcal{F}_{BA}}} \\ \mathcal{F}_{ST} &= (1 - e^{-\nu}) \rho^S(1 - \rho^T). \end{aligned} \quad (7)$$

f_{BA} is obtained by exchange $\rho_A \leftrightarrow \rho_B$ in (7). For antisymmetric rates (2)

$$\begin{aligned} j_{\text{asym}}^A(\rho^A, \rho^B) &= (\gamma - \epsilon_L)(e^{-\nu} - 1) f_{AB} f_{BA} + (\alpha - \alpha_L - \gamma + \epsilon_L)(1 - \rho^A) f_{AB} \\ &\quad + (\beta - \beta_L - \gamma + \epsilon_L) \rho^A f_{BA} + (\gamma - \epsilon_L) \rho^A(1 - \rho^A) \\ j_{\text{asym}}^B(\rho^A, \rho^B) &= -j_{\text{asym}}^A(\rho^B, \rho^A), \end{aligned} \quad (8)$$

f_{AB} being again given by (7).

3. SPREADING OF A LOCAL PERTURBATION

We shall study how an initial point-like excitation on the otherwise homogeneous stationary background propagates in the system. For our purposes it is convenient to adopt the quantum Hamiltonian formulation of the stochastic process. The method is reviewed in detail in ref. 1. In this

formulation, the state of our classic stochastic system of two chains of L sites is represented by a vector in a vector space,

$$|\Psi\rangle \in (\mathbb{C}^2)^{\otimes L} \otimes (\mathbb{C}^2)^{\otimes L}. \quad (9)$$

The stochastic dynamics is governed by a quantum Hamiltonian H acting in that vector space, $\partial |\Psi\rangle/\partial t = -H |\Psi\rangle$, with formal solution $|\Psi(t)\rangle = e^{-Ht} |\Psi(0)\rangle$. Stationary (i.e., time independent) states satisfy evidently $H |\Psi_{\text{stat}} = 0\rangle$. A particle on site k is represented by the vector $\binom{0}{1}$ and a vacancy by the vector $\binom{1}{0}$ at the relevant place in the tensor product (9). E.g., a system with only one particle on site $k=2$ on the A-chain and no particles on B-chain is represented as $|\Psi\rangle = \binom{1}{0} \otimes \binom{0}{1} \otimes \binom{1}{0}^{\otimes L-2} \otimes \binom{1}{0}^{\otimes L}$, etc. Given the state of the system $|\Psi\rangle$, the expectation value of particle density at site k on A-chain is computed by the analogue of the quantum-mechanical formula

$$\langle \hat{n}_k \rangle = \langle s | \hat{n}_k | \Psi \rangle \quad (10)$$

where $\langle s | = (1 \ 1 \ 1 \ \dots \ 1)$ is the row vector with all components 1, and \hat{n}_k is a local occupation number operator $\hat{n} = \begin{pmatrix} 0 & 0 \\ 0 & 1 \end{pmatrix}$ acting nontrivially at the k th subspace of the tensor product:

$$\hat{n}_k = (I^{\otimes k-1} \otimes \hat{n} \otimes I^{\otimes L-k}) \otimes I^{\otimes L}; \quad I = \begin{pmatrix} 1 & 0 \\ 0 & 1 \end{pmatrix}. \quad (11)$$

Analogously, the expectation value of particle density at site k on B-chain is computed by averaging operator $\hat{m}_k = I^{\otimes L} (I^{\otimes k-1} \otimes \hat{n} \otimes I^{\otimes L-k})$.

For our choice of the rates (4) there are no bulk correlations, all configurations with a fixed number of particles occur with the same probability (see (3), $\nu = 0$). Given the average particle and excitation dynamics in a driven diffusive two-channel system density ρ^Z on chain Z , the corresponding stationary state within the quantum Hamiltonian formalism is written as a product measure

$$|\rho^A \rho^B\rangle = \begin{pmatrix} 1 - \rho^A \\ \rho^A \end{pmatrix}^{\otimes L} \begin{pmatrix} 1 - \rho^B \\ \rho^B \end{pmatrix}^{\otimes L}, \quad (12)$$

meaning that there is a probability to find a particle on the A-chain $\langle \hat{n}_k \rangle = \rho^A$ and a hole $\langle I - \hat{n}_k \rangle = 1 - \rho^A$ at any site k , and $\langle \hat{m}_k \rangle = \rho^B$, $\langle I - \hat{m}_k \rangle = 1 - \rho^B$ for the B-chain.

We shall study the time evolution of the above homogeneous state in an infinite chain $-\infty < k < \infty$ perturbed at a single site $k = 0$:

$$|\Psi(0)\rangle = \left(1 + \Phi^A \frac{\hat{n}_0 - \rho^A}{\rho^A(1 - \rho^A)} + \Phi^B \frac{\hat{m}_0 - \rho^B}{\rho^B(1 - \rho^B)} \right) |\rho^A \rho^B\rangle, \quad (13)$$

where $|\rho^A \rho^B\rangle$ is a stationary state (12). Φ^A, Φ^B are constants, determining the strength and sign of perturbation at site 0. We shall see below that only the ratio Φ^A/Φ^B is important, hence we consider Φ^A, Φ^B to be sufficiently small for the averages (14) to be in a physical domain $0 \leq \langle \hat{n}_0 \rangle, \langle \hat{m}_0 \rangle \leq 1$. The density profile corresponding to this initial state is given by the average occupation numbers $\langle \hat{n}_k \rangle = \rho^A$, $\langle \hat{m}_k \rangle = \rho^B$ for all sites $k \neq 0$. At the site $k = 0$ the densities correspondingly are

$$\langle \hat{n}_0 \rangle = \rho^A + \Phi^A; \quad \langle \hat{m}_0 \rangle = \rho^B + \Phi^B. \quad (14)$$

The time evolution of the initial state (13) is given by a Hamiltonian $H^{(1)}$ of the stochastic process

$$\begin{aligned} |\Psi(t)\rangle &= e^{-Ht} |\Psi(0)\rangle \\ &= |\rho^A \rho^B\rangle + e^{-Ht} \left(\Phi^A \frac{\hat{n}_0 - \rho^A}{\rho^A(1 - \rho^A)} + \Phi^B \frac{\hat{m}_0 - \rho^B}{\rho^B(1 - \rho^B)} \right) |\rho^A \rho^B\rangle, \end{aligned} \quad (15)$$

where we used the stationarity of $|\rho^A \rho^B\rangle$: $H |\rho^A \rho^B\rangle = 0$.

Consider the quantity

$$S(t) = \frac{\langle \sum_k k(\hat{n}_k - \rho^A) \rangle}{\langle \sum_k (\hat{n}_k - \rho^A) \rangle} = \frac{1}{\Phi^A} \left\langle \sum_k k(\hat{n}_k - \rho^A) \right\rangle \quad (16)$$

which tracks the position of the center of mass of the excitation on A-chain. Denoting by δ the change of the center of mass position during the infinitesimal time interval τ , we have

$$\Phi^A \delta = \Phi^A (S(t + \tau) - S(t)) \approx \tau \frac{\partial}{\partial t} \sum_k k \langle \hat{n}_k \rangle = \tau \sum_k k \langle \hat{j}_{k-1}^A - \hat{j}_k^A \rangle \quad (17)$$

where we used the lattice continuity equation $\frac{\partial}{\partial t} \hat{n}_k = \hat{j}_{k-1}^A - \hat{j}_k^A$. Using the fact that far from the excitation there is an unperturbed state with a stationary flux $\langle \hat{j}_k^A \rangle = j^A$, one can shift the summation variable in (17) as

$$\sum_k k \langle \hat{j}_{k-1}^A - \hat{j}_k^A \rangle = \sum_k (k+1) \langle \hat{j}_k^A \rangle - \sum_k k \langle \hat{j}_k^A \rangle = \sum_k \langle \hat{j}_k^A - j^A \rangle. \quad (18)$$

Finally, it can be shown (see an Appendix B) that

$$\sum_k \langle j_k^A - j^A \rangle = \frac{\partial j^A}{\partial \rho^A} \Phi^A + \frac{\partial j^A}{\partial \rho^B} \Phi^B. \quad (19)$$

From (17) and (19) we have

$$\frac{\partial j^A}{\partial \rho^A} \Phi^A + \frac{\partial j^A}{\partial \rho^B} \Phi^B = \frac{\delta}{\tau} \Phi^A \equiv v_A \Phi^A, \quad (20)$$

where $v_A \equiv \frac{\delta}{\tau}$ is the collective velocity of the excitation on the A-chain. Repeating the calculations for the B-chain, we obtain:

$$\frac{\partial j^B}{\partial \rho^A} \Phi^A + \frac{\partial j^B}{\partial \rho^B} \Phi^B = v_B \Phi^B. \quad (21)$$

Now, if there is an interaction between the chains, the collective velocities must coincide, since the perturbation in one chain causes the response in the other and vice versa. Thus $v_B = v_A = v$, and one recognizes in (20, 21) the eigenvalue equation $\mathcal{D} |\Phi\rangle = v |\Phi\rangle$, where $|\Phi\rangle = \begin{pmatrix} \Phi^A \\ \Phi^B \end{pmatrix}$, and \mathcal{D} is the Jacobian $\mathcal{D}_{ik} = \partial j_i / \partial \rho_k$.

The solutions of the eigenvalue problem $v_1^{\text{coll}}, v_2^{\text{coll}}$ and the corresponding eigenfunctions $|\Phi_1\rangle, |\Phi_2\rangle$ have a transparent physical meaning. Namely, the center of mass of the initial perturbation Φ_r^A, Φ_r^B in the adjacent pair of sites will move with the velocity v_r^{coll} . An arbitrary initial perturbation $|\Phi\rangle$ will propagate along the *two* characteristics $v_1^{\text{coll}}t, v_2^{\text{coll}}t$. The conserved masses $\mathcal{M}_Z = \sum_k \langle \hat{n}_k^Z - \rho^Z \rangle$ of the splitted components will relate like α_1/α_2 where α_1, α_2 are expansion coefficients given by $|\Phi\rangle = \alpha_1 |\Phi_1\rangle + \alpha_2 |\Phi_2\rangle$.

Let us demonstrate the theory in the case of our stochastic model. The Jacobian $\mathcal{D}_{ik} = \partial j_i / \partial \rho_k$ is readily obtained from (5)

$$\mathcal{D} = \left(\begin{array}{cc} \frac{(1-2\rho^A)(1+(\beta-1)\rho^B)}{(\beta-1)\rho^B(1-\rho^B)} & \frac{(\beta-1)\rho^A(1-\rho^A)}{(1-2\rho^B)(1+(\beta-1)\rho^A)} \end{array} \right). \quad (22)$$

The collective velocities $v_1^{\text{coll}} > v_2^{\text{coll}}$ are the eigenvalues of \mathcal{D} . If $\beta = 0$, the eigenvalues and corresponding eigenvectors are given by:

$$v_1^{\text{coll}} = (1-\rho^A)(1-\rho^B); \quad \Phi_1 = \begin{pmatrix} 1 \\ -\frac{1-\rho^B}{1-\rho^A} \end{pmatrix}; \quad \beta = 0; \quad (23)$$

$$v_2^{\text{coll}} = 1-2\rho^A-2\rho^B+3\rho^A\rho^B; \quad \Phi_2 = \begin{pmatrix} 1 \\ \frac{\rho^B}{\rho^A} \end{pmatrix}; \quad \beta = 0. \quad (24)$$

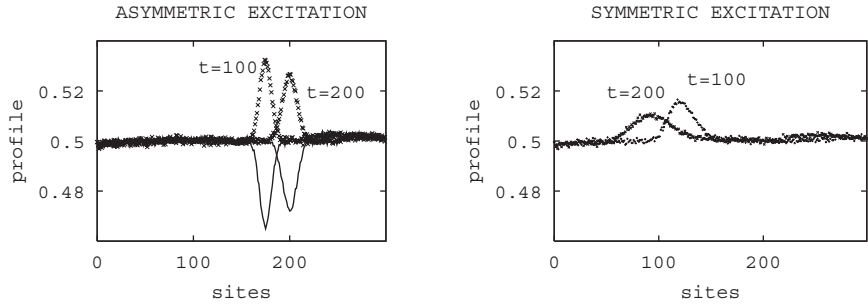


Fig. 2. Time evolution of a point-like initial perturbation $(+\delta, \pm\delta)$ on a 2-chain driven system. The parameters are: the background densities $\rho^A = \rho^B = 0.5$, $\beta = 0$. Left graph: at $t = 0$, the asymmetric perturbation $\delta\rho^A = -\delta\rho^B = 0.5$ is put at the middle site 150. The average density profiles after $t = 100$ and $t = 200$ Monte Carlo evolution steps are shown, averaged over $6 \cdot 10^5$ different histories. The component A is depicted with points and the component B with lines. Right graph: initial perturbation is symmetric $\delta\rho^A = \delta\rho^B = 0.5$. B-component evolution (not shown) is identical to the one of the A-component. The asymmetric perturbation moves with collective velocity 0.25 to the right, and the symmetric one to the left, in accordance with the theory (see Section 3).

Figure 2 shows the time evolution of the initially perturbed state (13) from Monte Carlo calculations, using random sequential update. The background densities are $\rho^A = \rho^B = 0.5$, which corresponds to $v_1^{\text{coll}} = -v_2^{\text{coll}} = 0.25$, $|\Phi_1\rangle = \begin{pmatrix} 1 \\ -1 \end{pmatrix}$, $|\Phi_2\rangle = \begin{pmatrix} 1 \\ 1 \end{pmatrix}$. Hence the initial asymmetric excitation (14) with $\Phi^A = -\Phi^B$ must spread to the right, and the symmetric excitation $\Phi^A = \Phi^B$ to the left with the collective velocities v_1^{coll} and v_2^{coll} respectively. This is precisely what is seen on the Fig. 2. An arbitrary excitation

$$\begin{pmatrix} \Phi^A \\ \Phi^B \end{pmatrix} = \frac{\Phi^A + \Phi^B}{2} \begin{pmatrix} 1 \\ 1 \end{pmatrix} + \frac{\Phi^A - \Phi^B}{2} \begin{pmatrix} 1 \\ -1 \end{pmatrix} \quad (25)$$

will split in two with the masses ratio $(\Phi^A - \Phi^B)/(\Phi^A + \Phi^B)$, spreading apart to the right and to the left from the origin.

4. SHOCK WAVES, RAREFACTION WAVES, AND THEIR COMBINATIONS

Now we ask the question: if we have prepared the system in a step function (shock) state with constant stationary backgrounds (ρ_L^A, ρ_L^B) and (ρ_R^A, ρ_R^B) at the left half space $k < 0$ and the right half space $k \geq 0$, respectively, what will happen with their interface?

Suppose interface will start moving. Due to mass conservation the Z -component of the interface should move with the velocity

$$V^Z(L, R) = \frac{j_R^Z - j_L^Z}{\rho_R^Z - \rho_L^Z} \tag{26}$$

where we used shortened notation $j_{L(R)}^Z = j^Z(\rho_{L(R)}^A, \rho_{L(R)}^B)$, and the $V^Z(L, R)$ marks the fact that the velocity is computed between the backgrounds “ L ” and “ R .” If $V^A(L, R) = V^B(L, R)$, the two interfaces evolve coherently, similar to the case discussed below (Fig. 4). If however $V^A(L, R) \neq V^B(L, R)$, then the incoherent motion in the A-chain will influence the B-chain and vice versa, destroying the interface. The possible way out for the system is to develop a plateau “ 0 ” in the middle, interpolating between the plateaus “ L ” and “ R ”, as shown on Fig. 4. Consequently, instead of one there will be two interfaces in each chain: the interface $L|0$ between “ L ” and “ 0 ” and the interface $0|R$. We must require the velocities in the A- and B-chains to be the same. The interface $L|0$ has the velocity

$$V(L, 0) = \frac{j^A(L) - j^A(0)}{\rho_L^A - \rho_0^A} = \frac{j^B(L) - j^B(0)}{\rho_L^B - \rho_0^B} \tag{27}$$

and analogously for the interface $0|R$

$$V(0, R) = \frac{j^A(R) - j^A(0)}{\rho_R^A - \rho_0^A} = \frac{j^B(R) - j^B(0)}{\rho_R^B - \rho_0^B}. \tag{28}$$

The solutions of Eqs. (27) and (28) define the location of possible middle plateau densities ρ_0^A, ρ_0^B . Since (27, 28) are nonlinear, they can have several solutions or no solutions at all. If a solution exists (see Fig. 3), one

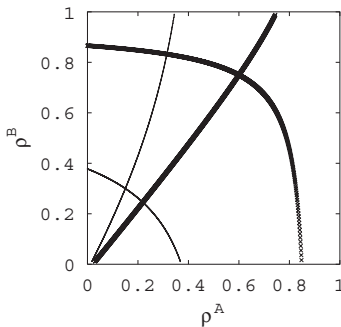


Fig. 3. Curves, showing locus of the points ρ_0^A, ρ_0^B , solving Eq. (27) with $\rho_1^A = 0.15, \rho_1^B = 0.3$ (thin curves) and Eq. (28) with $\rho_2^A = 0.6, \rho_1^B = 0.75$ (bold curves). $\beta = 0.2$. Crossings of the bold curves with the thin curves indicate possible solutions of (27, 28).

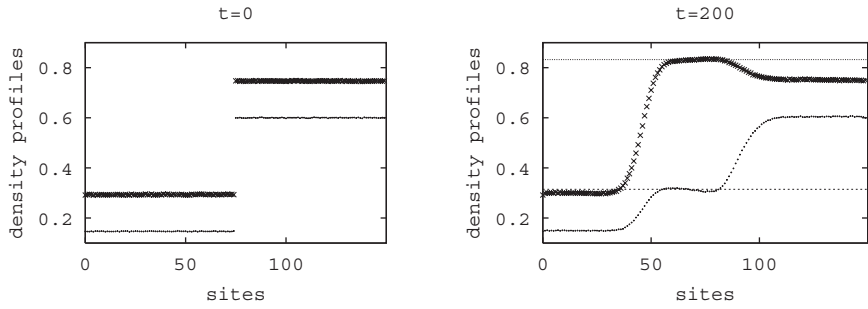


Fig. 4. Formation of a shock wave. Parameters are: $\beta = 0.2$. Left: the initial distribution: A-particles are distributed randomly with an average density 0.15 (0.6) on the left (on the right). Corresponding B-particles initial densities are 0.3 (0.75). Right: Result of Monte Carlo evolution after $t = 200$ Monte Carlo steps, averaged over $2 * 10^5$ different histories. The density profiles of A and B particles are depicted with points of different sizes, and the lines with theoretically expected middle shock values $\rho^A \approx 0.3146$, $\rho^B \approx 0.8323$ are drawn for comparison.

must require additionally $V(L, 0) < V(0, R)$ because the plateau “0” has to expand, and check the shock stability as discussed below.

In order to study the shock stability let us consider a shock of the form “ $L | 0 | R$ ” consisting of three consecutive plateaus at densities ρ_L^Z , ρ_0^Z and ρ_R^Z . A small deviation at the plateau “ K ” ($K = 0, L, R$) will split into two local excitations with the velocities $v_1^{\text{coll}}(K) > v_2^{\text{coll}}(K)$ as discussed in Section 3. In order for the shock to be stable, all local excitations have to be absorbed by the interfaces, that is,

$$v_1^{\text{coll}}(L), v_2^{\text{coll}}(L) > V(L, 0) > v_2^{\text{coll}}(0) \quad (29)$$

for the interface $L | 0$ and

$$v_1^{\text{coll}}(0) > V(0, R) > v_2^{\text{coll}}(R), v_1^{\text{coll}}(R) \quad (30)$$

for the interface $0 | R$. An example of such a double shock is shown on Fig. 4. The densities of particles ρ_0^A, ρ_0^B on the middle plateau satisfy Eqs. (27) and (28), which are graphically solved on Fig. 3. There are two solutions, one of which is realized (Fig. 4), while the other one violates $V(L, 0) < V(0, R)$. One can check that (29, 30) are satisfied.

If the second shock condition (30) is not satisfied, but instead one has

$$v_2^{\text{coll}}(0) < V(0, R) < v_2^{\text{coll}}(R), \quad v_1^{\text{coll}}(R); \quad v_1^{\text{coll}}(0) > V(0, R), \quad (31)$$

then the local perturbations will destroy the sharp interface, leading to a rarefaction wave connecting the plateaus $0 | R$, similar as discussed for one-component systems.^(1,7) An example of a rarefaction wave formation is

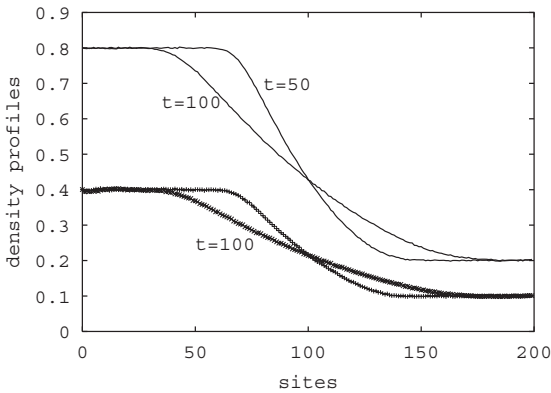


Fig. 5. Formation of a rarefaction wave. Parameters are: $\beta = 0$. The initial distribution is a Riemann step, with A-particles being distributed randomly with the average density 0.8(0.2) on the left (on the right). Corresponding B-particles initial densities are 0.4(0.1). The quantity (26) has here a meaning of the velocity of a mass transfer and is the same for both components $V^A(L, R) = V^B(L, R) = -0.08$, therefore only one wave is formed. The rarefaction wave condition (31) is satisfied. We show a result of Monte Carlo evolution after $t = 50, 100$ Monte Carlo steps, averaged over $2 * 10^5$ different histories.

shown on Fig. 5. The origin of conditions (30), (31) lies in the analytical properties of eigenvalues of the Jacobian $\mathcal{D}_{ik} = \partial j_i / \partial \rho_k$, that is, collective velocities $v_1^{\text{coll}}(l), v_2^{\text{coll}}(l)$, where l is a running coordinate along the curve defined by an average density profile $\rho^B(l)(\rho^A(l))$. An excellent discussion on the subject for the case of infinitesimally small shocks and rarefaction waves can be found in ref. 14.

One may ask what happens if neither shock-wave nor rarefaction-wave condition are satisfied. In this case a combination of both shock and rarefaction wave may be formed as illustrated on the example Fig. 6. There for simplicity we have taken symmetric initial conditions so that Eqs. (27, 28) are satisfied for arbitrary $\rho_0^A = \rho_0^B$. The velocity of the mass transfer (26) between the left (L) and right (R) plateaux respectively is the same for both chains $V^A(L, R) = V^B(L, R)$, but the collective velocities $v_1^{\text{coll}}(R), v_2^{\text{coll}}(R) < V(L, R)$ and $v_1^{\text{coll}}(L), v_2^{\text{coll}}(L) < V(L, R)$ satisfy neither the shock-type (30) nor the rarefaction-wave (31) criterion. As a result, a compromise is made: part of the profile with the high densities $\rho \in (\rho_L, \rho^*)$ develops a shock while for the small densities $\rho \in (\rho^*, \rho_R)$ the rarefaction wave is formed, see Fig. 6. Indeed for the interface $(\rho_L, \rho^* + \epsilon)$, $\epsilon \ll 1$, the shock condition analogous to (30) is satisfied while the interface $(\rho^* - \epsilon, \rho_R)$ satisfies respective rarefaction wave condition (31). The level $\rho^* = 0.525$ is

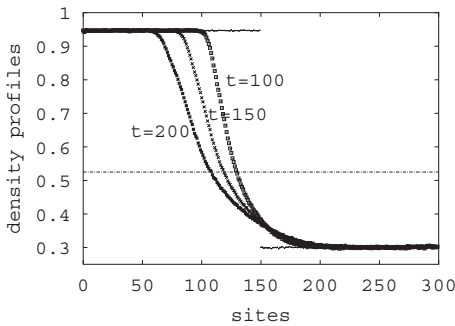


Fig. 6. Time evolution of a step-like initial profile, leading to shock wave and rarefaction wave coexistence. The parameters are: the left densities $\rho^A = \rho^B = 0.95$, the densities on the right $\rho^A = \rho^B = 0.3$, $\beta = 0$. The graph shows the average density profiles at $t = 0, 100, 150, 200$, symmetric in both components. Average over 10^5 histories is made. For the densities $\rho = \rho^* = 0.525$ and higher, the shock wave is formed, while for the lower densities $\rho < \rho^*$ one observes the rarefaction wave (see the end of Section 4 for details). The level $\rho = \rho^*$ is marked by a thin line.

defined by the crossing point $V(\rho_L, \rho^*) = v_2^{\text{coll}}(\rho^*)$ and can be predicted by hypothetical consideration of the initial condition as a sequence of small plateaus (shocks) at each level of density. All small shocks above $\rho = \rho^*$ condense in a single shock while those below ρ^* form the rarefaction wave. Similar analysis can be performed for other initial conditions. Note that for certain class of initial conditions we observe shocks of even more complicated structure. Their analysis will be presented elsewhere.

5. HYDRODYNAMIC LIMIT: COMPARISON WITH THE THEORY OF PARTIAL DIFFERENTIAL EQUATIONS

For most notions we have discussed in the framework of the stochastic particle system, one can find the respective analogies in the theory of partial differential equations (PDE). The naive continuum (Eulerian) limit of our stochastic dynamics on the lattice $\hat{n}_k(t) \rightarrow \rho^A(x, t)$, $\hat{m}_k(t) \rightarrow \rho^B(x, t)$ is a system of conservation laws

$$\frac{\partial \rho^Z(x, t)}{\partial t} + \frac{\partial j^Z(\rho^A, \rho^B)}{\partial x} = 0; \quad Z = A, B, \quad (32)$$

where j^Z is given by Eqs. (5)–(8). Here and below in this section we shall use $\rho^Z(x, t)$ for a continuously changing variable, not to be confused with

constant ρ^A, ρ^B from Section 3. Such systems of conservation laws are studied, e.g., in refs. 13 and 14.

The eigenvalues of the Jacobian $\frac{\partial j^i}{\partial \rho^k}$ (playing the role of collective velocities) are the characteristic velocities. For scalar conservation law $\partial \rho / \partial t + \partial j(\rho) / \partial x = 0$ with $\partial j(\rho) / \partial \rho = v(\rho)$ it follows that the line $x = v(\rho) t$, called characteristic, defines the space-time trajectory on which the local density $\rho(x, t)$ stays constant. For systems (32) of conservation laws, the situation is more complicated. However also there one can find two functions $w_i(\rho^A, \rho^B); i = 1, 2$, called Riemann invariants, which are constant along the respective characteristics $\frac{dx}{dt} = v_i$.⁽¹⁴⁾

Consider now a shock of the type drawn in Fig. 4. In the hydrodynamic limit, the interface region between the plateaus of constant densities will squeeze to a single point, giving rise to discontinuous change. Discontinuities in PDE theory are known to satisfy the so-called jump condition $v_s(\rho_+^Z - \rho_-^Z) = (j_+^Z - j_-^Z)$ where F_+ and F_- are the values of function F in the right and left edges of the discontinuity, and v_s is the speed of the propagation of the discontinuity. Comparing with (26) we recognize in v_s the shock velocity.

It is well known that an arbitrarily chosen smooth initial profile $\rho^Z(x, 0)$ will develop a singularity after finite time t .^(13, 14) To cure the singularity problem for the PDE, the simplest possible approach suggests adding a vanishing viscosity term ($\kappa \frac{\partial^2 \rho^Z}{\partial x^2}; \kappa \rightarrow 0$) to the right-hand side of (32). This is enough to avoid singularities and by numerical integration we find that this regularization term leads to the correct answer for the initial Riemann problem, as compared to the stochastic model.

Another possibility to obtain a viscosity term is to average exact lattice continuity equations of the stochastic process

$$\frac{\partial}{\partial t} \hat{n}_k = \hat{j}_{k-1}^A - \hat{j}_k^A \tag{33}$$

$$\frac{\partial}{\partial t} \hat{m}_k = \hat{j}_{k-1}^B - \hat{j}_k^B \tag{34}$$

for occupation number operators $\langle \hat{n}_k \rangle \rightarrow \rho^A(x, t)$, $\langle \hat{m}_k \rangle \rightarrow \rho^B(x, t)$, allowing for continuous change of space $k, k+1 \rightarrow x, x+dx$. For the case (4), the flux operator \hat{j}_k^A can be obtained from the general expression (A.1) and it reads

$$\hat{j}_k^A = \hat{n}_k(1 - \hat{n}_{k+1}) \left(1 + \frac{\beta - 1}{2} (\hat{m}_k + \hat{m}_{k+1}) \right). \tag{35}$$

j_k^B is obtained by an exchange $\hat{n} \leftrightarrow \hat{m}$ in the above. We substitute (35) into (33), (34), average, factorize and Taylor expand the latter with respect to site spacing dx as, e.g., $\langle \hat{m}_{k+1} \rangle = \rho^B(x, t) + dx \frac{\partial \rho^B(x, t)}{\partial x} + (dx^2/2) \frac{\partial^2 \rho^B(x, t)}{\partial x^2} + \dots$. Keeping the terms up to dx^2 in the expansion, we obtain

$$\frac{\partial \rho^A}{\partial t'} + \frac{\partial j^A(\rho^A, \rho^B)}{\partial x} = \kappa \frac{\partial}{\partial x} \left((1 + (\beta - 1) \rho^B) \frac{\partial \rho^A}{\partial x} \right) \quad (36)$$

$$\frac{\partial \rho^B}{\partial t'} + \frac{\partial j^B(\rho^A, \rho^B)}{\partial x} = \kappa \frac{\partial}{\partial x} \left((1 + (\beta - 1) \rho^A) \frac{\partial \rho^B}{\partial x} \right) \quad (37)$$

$$\kappa = \frac{dx}{2} \rightarrow 0; \quad \frac{\partial}{\partial t} = 2\kappa \frac{\partial}{\partial t'}. \quad (38)$$

where $j^Z(\rho^A, \rho^B)$ are given by the (5).

We found by a numerical integration of (36), (37) that also here the correct result are obtained for the step-function initial conditions. It seems therefore that the choice of viscosity matrix is rather arbitrary, if initial step-function conditions are chosen. However, the PDE becomes more sensitive if solved on a finite interval with fixed boundary values. In this setting, the choice of viscosity is important, since different choices give different answers. The details will be published elsewhere.

6. CONCLUSION

To conclude, we have studied a two lane particle exclusion process on the microscopic level, focusing on the temporal behaviour of the elementary local excitations, domain walls (shocks) and rarefaction waves. By analyzing the flow of localized excitations and calculating their collective velocities we derived a criterion for the stability of shocks, somewhat analogous to our recent analysis of systems with a single conservation law.⁽¹⁾ However, unlike in systems with a single conservation law, shocks generically come in pairs, since the two conserved densities give rise to two distinct collective velocities. Because of the interaction between the chains, or more generally, between the two conserved densities, these velocities are the eigenvalues of the Jacobian of the current-density relation. The eigenvectors of the Jacobian parametrize the expansion of the strength of a generic excitation into the two eigenmodes of the systems. These eigenmodes (corresponding to the special case of a single excitation) correspond to a special tuning of the strength of the excitation in each conserved density: The relative strength for an eigenmode with fixed collective velocity is the

ratio of the components of the corresponding eigenvector. Initial profiles not satisfying the stability criterion for shocks evolve into rarefaction waves or more complicated structures. Since nowhere in our analysis we make use of the specific properties of our model we argue that as in systems with a single conservation law, all the properties discussed above can be derived from the macroscopic current, irrespective of the microscopic details of the model.

Going one step further we take a naive continuum limit (Euler scale) to obtain a system of coupled nonlinear PDE's. Thus we obtain a microscopic interpretation for the characteristics (as flow of localized perturbations) and for the jump condition for shock solutions. Monte Carlo simulation of the model as well as numerical integration of the PDE's suggest that the uniqueness problem for the Riemann problem can be resolved by using a quite arbitrary viscosity matrix with vanishing viscosity. However, for the stationary solution with fixed boundary values the problem appears to be more intricate. A detailed analysis is necessary and will be presented in future work. The hydrodynamic limit of another family of lattice gas models with two conservation laws, differing from ours by internal symmetries, has been studied recently.⁽⁸⁾ They give rise to a different set of PDE's, but we believe that our analysis can be applied to this family as well. On the other hand we also expect that the mathematically rigorous work of ref. 8 can be generalized to models of the type considered here.

APPENDIX A. CURRENT-DENSITY RELATION IN THE GENERAL CASE

By definition, the stationary flux is written as sum of the hopping rates times the stationary probabilities Ω of the corresponding local configurations, see Fig. 1:

$$j^A(\rho^A, \rho^B) = \alpha\Omega(\circ\circ) + \beta\Omega(\bullet\circ) + \gamma\Omega(\bullet\bullet) + \epsilon\Omega(\circ\bullet) \\ - \alpha_L\Omega(\circ\circ) - \beta_L\Omega(\bullet\bullet) - \gamma_L\Omega(\circ\bullet) - \epsilon_L\Omega(\bullet\circ). \quad (\text{A.1})$$

Here we introduced the short notation $\Omega(\circ\circ)$ for the probability to find the configuration with one particle (filled circle \bullet) and 3 holes (empty circle \circ), arranged like in Fig. 1, first configuration on the upper row), in a steady state with average densities ρ^A and ρ^B . Analogously, $\Omega(\bullet\bullet)$ is the probability to find 3 particles, 1 hole as in Fig. 1, second configuration on upper row. In terms of occupation number operators \hat{n}_k, \hat{m}_k for chains A (bottom circles) and B (upper circles),

$$\Omega(\bullet\bullet) = \langle \hat{n}_k(1 - \hat{n}_{k+1}) \hat{m}_k \hat{m}_{k+1} \rangle, \quad (\text{A.2})$$

and so on. If the rates satisfy (1) and (2) in the symmetric and antisymmetric case respectively, then the correlation function can be factorized due to (3), e.g.,

$$\langle \hat{n}_k(1 - \hat{n}_{k+1}) \hat{m}_k \hat{m}_{k+1} \rangle = \langle \hat{n}_k \hat{m}_k \rangle \langle (1 - \hat{n}_{k+1}) \hat{m}_{k+1} \rangle = \rho^B \langle \hat{n}_k \hat{m}_k \rangle - \langle \hat{n}_k \hat{m}_k \rangle^2. \quad (\text{A.3})$$

Above we used the translational invariance and the fact that $\langle \hat{m}_k \rangle = \rho^B$, $\langle \hat{n}_k \rangle = \rho^A$. Factorizing Eq. (A.1), and using (1), (2), one obtains

$$j^A(\rho^A, \rho^B) = K \Omega(\circ) \Omega(\bullet) + (1 - \rho^A)(\alpha - \alpha_L - \gamma + \epsilon_L) \Omega(\circ) + \rho^A(\beta - \beta_L - \gamma + \epsilon_L) \Omega(\bullet) + \rho^A(1 - \rho^A)(\gamma - \epsilon_L)$$

where

$$K = -\alpha + \alpha_L - \beta + \beta_L + \epsilon + \gamma - \epsilon_L - \gamma_L = \begin{cases} (\epsilon - \gamma_L)(e^\gamma - 1), & \text{symmetric case} \\ (\gamma - \epsilon_L)(e^{-\gamma} - 1), & \text{antisymmetric case.} \end{cases} \quad (\text{A.4})$$

Finally, $\Omega(\circ) = \langle \hat{n}_k(1 - \hat{m}_k) \rangle$ can be calculated directly from the stationary distribution (3) which after some algebra gives the expression (7). $\Omega(\bullet)$ is obtained from (7) by exchanging $\rho^A \leftrightarrow \rho^B$.

APPENDIX B. PROOF OF EQ. (11)

Consider $\mathcal{L} = \sum_k \langle \hat{j}_k^A - j^A \rangle$, which is by definition

$$\mathcal{L} = \sum_k \langle s | (\hat{j}_k^A - j^A) e^{-Ht} \left(1 + \Phi^A \frac{\hat{n}_0 - \rho^A}{\rho^A(1 - \rho^A)} + \Phi^B \frac{\hat{m}_0 - \rho^B}{\rho^B(1 - \rho^B)} \right) | \rho^A \rho^B \rangle \quad (\text{B.1})$$

$\langle s |$ is the constant row vector (1 1 1...1) (see ref. 1 for details). First, $\langle s | \hat{j}_k^A | \rho^A \rho^B \rangle = j^A$ by the definition of the stationary flux. Thus (B.1) is simplified as

$$\mathcal{L} = \sum_k \langle s | \hat{j}_k^A e^{-Ht} \Phi^A \frac{\hat{n}_0 - \rho^A}{\rho^A(1 - \rho^A)} | \rho^A \rho^B \rangle + \langle s | \hat{j}_k^A e^{-Ht} \Phi^B \frac{\hat{m}_0 - \rho^B}{\rho^B(1 - \rho^B)} | \rho^A \rho^B \rangle. \quad (\text{B.2})$$

Due to translational invariance, the above expression can be rewritten as

$$\sum_k \langle s | \hat{j}_0^A \Phi^A e^{-Ht} \frac{\hat{n}_k - \rho^A}{\rho^A(1-\rho^A)} |\rho^A \rho^B\rangle + \langle s | \hat{j}_0^B \Phi^B e^{-Ht} \frac{\hat{m}_k - \rho^B}{\rho^B(1-\rho^B)} |\rho^A \rho^B\rangle. \quad (\text{B.3})$$

Because the total number of particles in each chain is conserved, the Hamiltonian H commutes with $\sum_k \hat{n}_k, \sum_k \hat{m}_k$. Using this, and the fact that the $|\rho^A \rho^B\rangle$ is stationary, the term e^{-Ht} can be deleted from (B.3). Substituting the definition of $|\rho^A \rho^B\rangle$ from (12) into the expression below, we have

$$\begin{aligned} & \sum_k (\hat{n}_k - \rho^A) |\rho^A \rho^B\rangle \\ &= \sum_k \begin{pmatrix} 1-\rho^A \\ \rho^A \end{pmatrix}^{\otimes k-1} \left[\begin{pmatrix} -\rho^A & 0 \\ 0 & 1-\rho^A \end{pmatrix} \begin{pmatrix} 1-\rho^A \\ \rho^A \end{pmatrix} \right] \begin{pmatrix} 1-\rho^A \\ \rho^A \end{pmatrix}^{\otimes L-k-1} \begin{pmatrix} 1-\rho^B \\ \rho^B \end{pmatrix}^{\otimes L} \\ &= \rho^A(1-\rho^A) \frac{\partial}{\partial \rho^A} |\rho^A \rho^B\rangle. \end{aligned} \quad (\text{B.4})$$

Here we have used the explicit representation of the particle number operator $\hat{n} = \begin{pmatrix} 0 & 0 \\ 0 & 1 \end{pmatrix}$. Analogously, $\sum_k (\hat{m}_k - \rho^B) |\rho^A \rho^B\rangle = \rho^B(1-\rho^B) \frac{\partial}{\partial \rho^B} |\rho^A \rho^B\rangle$. Substituting this together with (B.4) in (B.3) we obtain Eq. (19).

Note the specific fact that the stationary state in our system is a product measure (12). However the validity of the result (19) extends to a much wider class of driven systems with short-ranged correlations.

ACKNOWLEDGMENTS

We thank M. Salerno, B. Tóth, and C. Bahadoran for fruitful discussions. GMS acknowledges financial support from DAAD in the framework of the PROBRAL programme.

REFERENCES

1. G. M. Schütz, Exactly solvable models for many-body systems far from equilibrium, in *Phase Transitions and Critical Phenomena*, Vol. 19, C. Domb and J. Lebowitz, eds. (Academic Press, London, 2000).
2. J. Krug., Boundary-induced phase transitions in driven diffusive systems, *Phys. Rev. Lett.* **67**:1882–1885 (1991).
3. M. R. Evans, D. P. Foster, C. Godrèche, and D. Mukamel, Symmetric exclusion model with two species: Spontaneous symmetry breaking, *J. Stat. Phys.* **80**:69–102 (1995).
4. F. Rezakhanlou, Hydrodynamic limit for attractive particle systems in Z^d , *Comm. Math. Phys.* **140**:417–448 (1991).

5. M. V. Freore, H. Guiol, K. Ravishankar, and E. Saada, Microscopic structure of the step exclusion process, *Bull. Braz. Math. Soc.* **33**:25–45 (2002).
6. A. B. Kolomeisky, G. M. Schütz, E. B. Kolomeisky, and J. P. Straley, Phase diagram of one-dimensional driven lattice gases with open boundaries, *J. Phys. A* **31**:6911–6921 (1998).
7. V. Popkov and G. M. Schütz, Steady-state selection of driven diffusive systems with open boundaries, *Europhys. Lett.* **48**:257–263 (1999).
8. B. Tóth and B. Valkó, to be published.
9. V. Popkov and I. Peschel, Symmetry breaking and phase coexistence in a driven diffusive two-channel system, *Phys. Rev. E* **64**:026126 (2001).
10. B. Derrida, S. A. Janowsky, J. L. Lebowitz, and E. R. Speer, Exact solution of the totally asymmetric simple exclusion process: Shock profiles, *J. Stat. Phys.* **73**:813–842 (1993).
11. B. Derrida, M. R. Evans, V. Hakim, and V. Pasquier, Exact solution of a 1D asymmetric exclusion process using a matrix formulation, *J. Phys. A* **26**:1493 (1993); G. Schütz and E. Domany, Phase transitions in an exactly soluble one-dimensional exclusion process, *J. Stat. Phys.* **72**:277–297 (1993).
12. T. M. Liggett, *Stochastic Interacting Systems: Contact, Voter and Exclusion Processes* (Springer, Berlin, 1999).
13. D. Serre, *Systems of Conservation Laws* (Cambridge University Press, 1999).
14. P. D. Lax, *Hyperbolic Systems of Conservation Laws and the Mathematical Theory of Shock Waves* (Society for Industrial and Applied Mathematics, Philadelphia, PA, 1973).